Physics Letters A 381 (2017) 2250–2255

Contents lists available at ScienceDirect

Physics Letters A

www.elsevier.com/locate/pla

Discussion

Nonlinear dynamics and bifurcation mechanisms in intense electron beam with virtual cathode

Nikita S. Frolov [a,b,*], Semen A. Kurkin [a,b], Alexey A. Koronovskii [b,a], Alexander E. Hramov [a,b]

[a] Yuri Gagarin State Technical University of Saratov, 77 Politechnicheskaya str., Saratov, 410054, Russia
[b] Saratov State University, 83 Astrakhanskaya str., Saratov, 410012, Russia

ARTICLE INFO

Article history:
Received 30 November 2016
Received in revised form 11 May 2017
Accepted 14 May 2017
Available online 19 May 2017
Communicated by F. Porcelli

Keywords:
Nonlinear dynamics
Spatiotemporal chaos
Pattern formation
Bifurcations
Electron beam
Virtual cathode

ABSTRACT

In this paper we report on the results of investigations of nonlinear dynamics and bifurcation mechanisms in intense electron beam with virtual cathode in micrometer-scaled source of sub-THz electromagnetic radiation. The numerical analysis is provided by means of 3D electromagnetic particle-in-cell (PIC) simulation. We have studied evolution of the system dynamics with the change of beam current value by means of Fourier and bifurcation analysis. The bifurcation diagram has identified a number of the alternating regions of beam current with regular or chaotic regimes of system dynamics. The study of spatiotemporal dynamics of formed electron structures in the beam has revealed the physical mechanisms responsible for the regimes switchings in the system.

© 2017 Elsevier B.V. All rights reserved.

1. Introduction

Spatially extended dynamical systems attract great attention of scientific community as they are able to demonstrate a large number of nonlinear wave phenomena and processes [1–4]. The most significant among others are formation of patterns, coherent structures and development of spatiotemporal chaos. Investigation of mentioned nonlinear phenomena and their properties in the spatially extended media helps researchers to understand the nature of complex processes taking place in the real physical systems.

Analysis of nonlinear dynamics has traditionally a great importance for such fields of modern science as microwave and terahertz (THz) electronics where microwave and THz oscillators exhibit properties of spatially extended dynamical systems [5–11]. In this sense both vacuum electron and solid state devices demonstrate a number of interesting and important nonlinear features. The example of solid-state device that has properties of nonlinear active medium is the semiconductor superlattice (SSL) — prospective solid-state source of THz radiation [12–14]. In a recently published paper the dynamics of SSL has been studied in the framework of bifurcation analysis [15]. It has been also found out that a number of unexpected nonlinear phenomena emerge while coupling SSL to the external resonator [5].

Beam-plasma systems also demonstrate behavior being peculiar to active nonlinear media and, as a consequence, the study of nonlinear dynamics of intense electron beams is of particular interest at present time. Intense electron beams drifting in vacuum tubes, from the viewpoint of collective dynamics of charged particles, show a variety of nonlinear phenomena including chaotic dynamics and patterns formation [16,17,6–9,18,11]. It is well-known that as a beam current exceeds the space-charge limiting current, I_{SCL}, the moving intense beam loses its stability and performs spatiotemporal oscillations [19–23]. These oscillations are caused by the formation in the beam of the non-stationary electron pattern, the so-called virtual cathode (VC), — the coherent electron structure that represents a dense cloud of charged particles and limits the propagation of the most parts of the beam. This effect of virtual cathode formation is used in high-power microwave devices called “Vircators” [19,20,24,25,23]. Virtual cathode oscillations usually have a complex form (often relaxation-like) due to the collective interaction of a large number of charged particles with self-consistent electric field and the presence of the internal electron feedback. The dynamics of VC is known to be sensitive to the variation of the control parameters, particularly, the beam current and energy [31,26–28,6,29,30]. Variations of the

* Corresponding author at: Yuri Gagarin State Technical University of Saratov, 77 Politechnicheskaya str., Saratov, 410012, Russia.
E-mail address: phrolovns@gmail.com (N.S. Frolov).

http://dx.doi.org/10.1016/j.physleta.2017.05.031
0375-9601/© 2017 Elsevier B.V. All rights reserved.

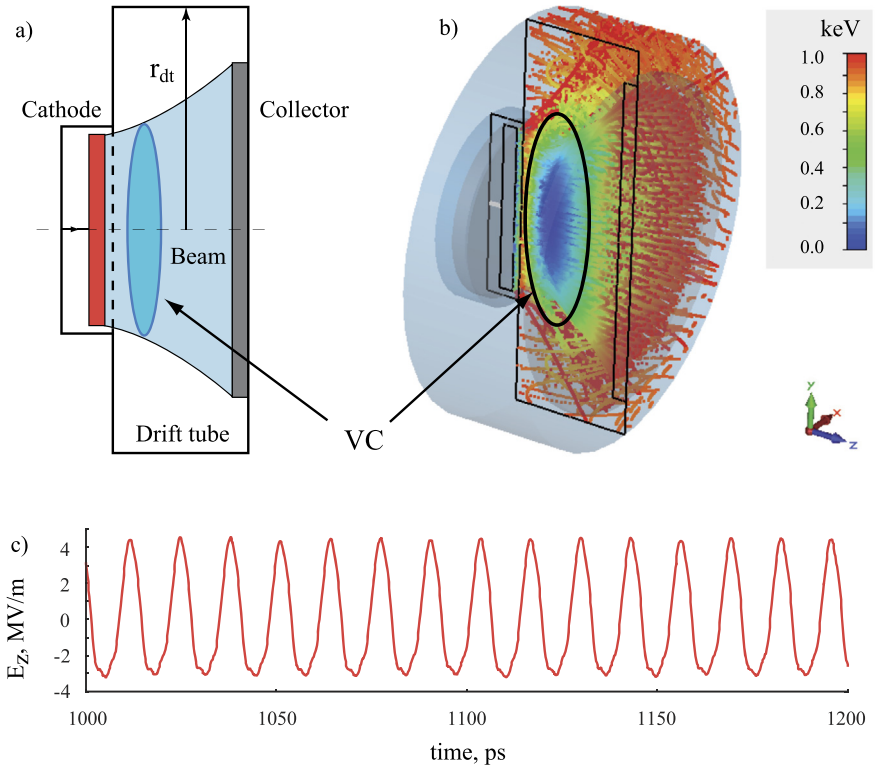

Fig. 1. (*a*) Schematic view of nanovircator with electron beam. Electron beam is highlighted with blue. It drifts from the cathode area (red brick) to the collector (gray brick) through the cylindrical drift tube of radius r_{dt}. (*b*) Cross-section view of the considered system in CST Particle Studio 2016. The region of the dense electron structure is denoted as "VC". Here, the charged particles are colored according to the value of their energy. (*c*) Typical time series of electric field relaxation-like oscillations in the VC area, $I_0 = 2.52$ A. (For interpretation of the references to color in this figure legend, the reader is referred to the web version of this article.)

control parameters provide rich set of complex nonlinear phenomena including pattern formation and regimes of spatio-temporal chaos [31–36].

In this paper we present the results of investigations of dynamics of the spatially extended system comprising the intense electron beam with the overcritical current and perform the analysis of mechanisms of the transition to chaos and the formation and destruction of coherent structures in such system. This study has been carried out in the framework of consideration of the "nanovircator" model — micrometer-scaled source of sub-THz electromagnetic radiation [37–39]. The choice of this model is determined by the growing interest to the research and development of compact sources of broadband sub-THz and THz radiation [40,23]. Besides, a systematic study of electron beam behavior and mechanisms of a chaotic oscillations in "nanovircator" has not been held so far. Moreover, the obtained results reveal the general properties of the intense electron beam dynamics in the vircator systems without the external magnetic field.

2. Nanovircator model and simulation details

We examine a dynamics of the overcritical electron beam with the help of the well-proven numerical 3D electromagnetic PIC-simulation tool [41,42] — CST Particle Studio (CST PS) 2016 licensed software [43]. It is based on the self-consistent solution of Maxwell's equations by means of finite-difference time-domain (FDTD) method and relativistic motion equations that describe particles behavior [42,44,45]. FDTD method is based on the discretization of Maxwell's equations written in differential form in Cartesian coordinate system. In this case, the meshes for the fields E and H are shifted relative to each other by half the step of the discretization of time and each of the spatial variables; such a complex grid is called Yee grid [46]. Maxwell's finite-difference equations make it possible to determine the fields E and H at a given time step based on the known values of the fields in the previous step. So, CST PS computes the electromagnetic fields according to Maxwell's equations to give a solution to the equation of motion for the particles [52]. This allows the evaluation of the Lorentz force in an explicit time-domain scheme where the time step is controlled by the size of the mesh grid in accordance with the Courant–Friedrichs–Lewy condition [47]. The particle movement imprints a current density that is written back into Maxwell's equation allowing the current and charge conservation. In order to accurately discretize the geometry of the different objects constituting the whole structure, CST PS uses a hexahedral grid with a perfect description of rounded solids, the so-called perfect boundary approximation (PBA) [48].

For more information about mathematical and numerical methods used in CST PS see Ref. [43]. The accuracy and efficiency of calculations via CST PS are proved by both solving test electromagnetic problems and simulation of different types of microwave devices and its components [49–52,25].

The schematic view and visualization in three dimensions of the system investigated in CST PS are presented in Fig. 1. One can see, that the electron active medium is formed in this system as a concentration of particles emitted from the cathode surface and propagating to the collector through the drift tube. We considered the short drift tube with length $L = 0.15$ mm and radius $r_{dt} = 0.28$ mm to realize the fast transition to the non-equilibrium state of the electron beam in this system. The detailed description of "nanovircator" geometry is given in Ref. [37]. The external magnetic field equals to zero.

Taking into account the given geometrical parameters and according to Bogdankevich–Rukhadze law [21], the non-stationary electron structure, VC, is formed in the electron beam at current $I_{SCL} = 2.25$ A for the beam initial energy $U_0 = 1.0$ keV. Note,

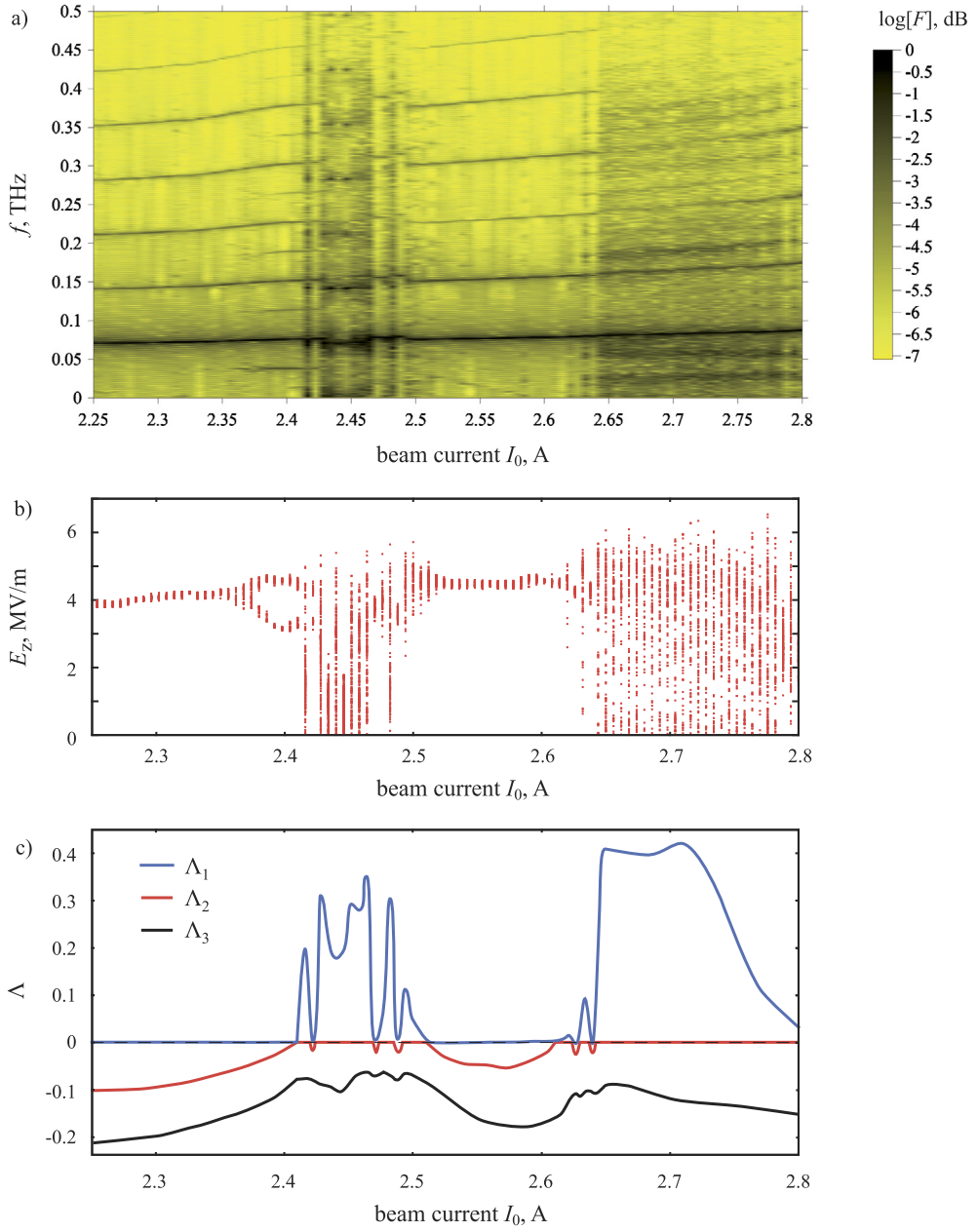

Fig. 2. (*a*) Evolution of log-scaled Fourier spectrum of oscillations of the electric field longitudinal component (log[F]) with the change of beam current value $I_0 > I_{SCL}$. (*b*) Bifurcation diagram representing the behavior of the electric field oscillations maxima with the change of beam current value ($I_0 > I_{SCL}$). (*c*) Dependencies of the three highest Lyapunov exponents Λ estimated from the $E_z(t)$ oscillations time series on the beam current value I_0.

the frequency of VC oscillations, f_{VC}, is close to the effective beam plasma frequency [53], f_p, that depends on the beam space-charge density and, consequently, beam current. The estimation of the plasma frequency for the described set of system parameters shows that the VC oscillation frequency lies within the range 70–95 GHz.

We have monitored oscillations of the electric field longitudinal component E_z in the area of VC to provide a bifurcation analysis and to study the physical mechanisms of the transition to chaos in the investigated spatially extended electron system — nanovircator. In our work, we have used *Field Probe* tool [43] located on the beam propagation axis at the distance 0.035 mm from the grid to measure the electric field oscillations in the area of VC. We have also examined the space-charge density $\rho(z,t)$ dynamics to find the correlation between the processes of electron pattern transformations and the observed bifurcations.

3. Main results

We have studied the evolution of nanovircator dynamics with the change of the beam current value, I_0. We have chosen I_0 as the key control parameter for this dynamical system, as it is known to have the strongest influence on intense electron beam behavior, especially in the regimes of VC formation [6,17].

It is more expedient to examine the complex dynamics of the nanovircator analyzing the oscillations of electric field in the VC area. In Fig. 2 the evolution of log-scaled Fourier spectrum of electric field oscillations log[F] (a) is shown and accompanied by the bifurcation diagram (b) and the dependency of the three highest Lyapunov exponents Λ_1, Λ_2 and Λ_3 on the beam current I_0 (c) determined from the time series of electric field oscillations according to the Wolf et al. algorithm [54]. The beam current is

varied here from the minimal value I_{SCL} determined by the appearance of VC in the system to the maximum achievable current determined by the electron emission density. One can see that the electric field oscillations are characterized by a number of higher harmonics of fundamental frequency f_{VC} in the spectrum. This is related with the relaxation character of VC oscillations caused by the relatively long period of space charge accumulation in the VC area and rather fast discharge (see Fig. 1(c)). It is also easy to see the almost linear growth of the VC fundamental frequency f_{VC} and its higher harmonics with the increase of the beam current, I_0. It is well-known that f_{VC} is proportional to the electron beam plasma frequency f_p [23,53]. So, such behavior of f_{VC} is the consequence of the linear dependency of the electron beam plasma frequency on the beam current: $f_p \sim I_0$. The most significant phenomenon given in Fig. 2 is the alternation of periodic and chaotic regimes of system dynamics. According to the figure, it is easy to detect two areas of nanovircator complex behavior: the first of them corresponds to $2.41\,\text{A} < I_0 < 2.47\,\text{A}$ and the second — $2.64\,\text{A} < I_0 < 2.8\,\text{A}$.

One can also check the presence of periodic and chaotic dynamics of the considered electron system with VC while comparing directly the evolution of Fourier spectrum with the bifurcation diagram presented in Fig. 2(b) and the three highest Lyapunov exponents behavior in Fig. 2(c). The bifurcation diagram characterizes the dynamics of the considered system under variation of the control parameter I_0 in terms of distribution of the electric field oscillations maxima. The diagram shows that the maxima of the electric field oscillations are concentrated in the very narrow region at low values of I_0 that corresponds to the regular oscillatory behavior of the nanovircator. It is also confirmed by the highest Lyapunov exponent which equals to zero and the second and third Lyapunov exponents which are both negative in this area. The regions of I_0 where the spectra of the electric field oscillations correspond to chaotic dynamics are characterized by the positive values of the highest Lyapunov exponents and by the significantly wider and more complex distributions of the maxima in the bifurcation diagram. One can observe in Fig. 2(b) the period-doubling bifurcation at $I_0 = 2.37\,\text{A}$ that foreruns the transition from regular to chaotic oscillations of VC in the system. Notable, that there are narrow windows of regular behavior, namely at $I_0 = 2.422\,\text{A}$, $I_0 = 2.47\,\text{A}$ and $I_0 = 2.488\,\text{A}$ which are characterized by zero value of Λ. The chaotic dynamics switches to regular one with the further growth of beam current at $I_0 \approx 2.5\,\text{A}$. Next abrupt transition to chaotic VC oscillations takes place at $I_0 \approx 2.63\,\text{A}$.

In this respect we have addressed to ourselves the question: what physical processes take place in the intense electron beam with VC underlying the described bifurcations? To answer this question we have carried out the detailed investigations of the pattern formation processes in the considered electron medium due to the collective interactions of large number of charged particles.

The Fourier spectra and phase portraits of longitudinal electric field E_z oscillations illustrating the dynamical regimes of VC in the nanovircator are presented in Fig. 3 for the different values of I_0 corresponding to five characteristic regions of the beam current with the different types of oscillatory dynamics. These plots are also accompanied by the corresponding spatiotemporal distributions of the electron beam space charge density $\rho(z,t)$ in the system. So, we can relate the certain dynamical regime of the nanovircator to the features of coherent electron structures formation or destruction.

To illustrate the dynamics of the electron beam at low current values $I_0 = 2.25 \div 2.36\,\text{A}$ where $\Lambda = 0$, we have picked the value of beam current from this range, namely $I_0 = 2.3\,\text{A}$. The characteristics of electron beam oscillations are presented in Fig. 3(a). It is clearly seen that the spectrum of E_z oscillations consists of the well-defined fundamental frequency f_{VC} and its higher harmonics, the phase portrait corresponds to noisy periodic solution. The origin of the noise may be related with discrete particle noise of PIC simulation algorithm. The regular spatiotemporal behavior of well-formed VC in the electron beam corresponds to this dynamical regime. Notable, that in the observed region of I_0 values VC consists of the only one electron cloud where the maximal space charge is concentrated.

Further, the system passes through the period-doubling bifurcation at $I_0 \approx 2.37\,\text{A}$ and the double-period oscillation regime with $\Lambda_1 = 0$ and $\Lambda_{2,3} < 0$ exists within the range $2.37\,\text{A} < I_0 < 2.41\,\text{A}$ (see Fig. 2). Fig. 3(b) illustrates electron beam behavior at $I_0 = 2.4\,\text{A}$. One can see that period-doubling bifurcation causes the appearance of satellites around the fundamental frequency f_{VC} and its higher harmonics. The attractor of this dynamical regime represents the doubled limit cycles. In terms of the electron pattern dynamics, the formation of the doubled limit cycle is determined by the splitting of single electron structure (VC) into two stable simultaneously oscillating bunches (VCs) that occurs at certain (bifurcation) beam current value because of the increased space charge forces. Note, that the second electron structure is formed closer to the injection plane than the initial one, in the reflected part of the beam. These electron bunches oscillate with the slightly different frequencies, according to the different values of the space charge density in these structures and, as a consequence, the dynamics of the entire system corresponds to double-period oscillations.

Next bifurcation at $I_0 = 2.41\,\text{A}$ leads to the transition to chaotic dynamics. We illustrate chaotic beam dynamics at $I_0 = 2.45\,\text{A}$, where $\Lambda_1 = 0.293$, $\Lambda_2 = 0$, $\Lambda_3 = -0.09$. Chaotic behavior occurs due to a loss of stability of the configuration with two electron bunches in the system. Actually, the influence of the bunches on each other dynamics through the space charge forces increases with the beam current growth and becomes critical at the bifurcation value of I_0. As a result, one can observe the complex interaction between two electron structures (VCs) that determines chaotic behavior of the beam and the high level of noise components in the spectrum of E_z oscillations. Such dynamics of the system exists in a rather wide range of the beam currents $2.41\,\text{A} < I_0 < 2.5\,\text{A}$.

Electron beam switches again to the regular oscillations regime at $I_0 \approx 2.5\,\text{A}$ (Fig. 3(d)) due to the destruction of one of the electron bunches under the influence of the increased Coulomb repulsion forces. Again, there is only one electron structure (VC) in the system in that case. It makes regular oscillations similar to the regime in Fig. 3(a); the main difference is that VC is formed closer to the injection plane in the case in Fig. 3(d) owing to the increased space charge density value in this situation of the greater beam current. Such regular regime exists within the range $2.5\,\text{A} < I_0 < 2.63\,\text{A}$.

The abrupt transition to the chaotic oscillations occurs in the system when the beam current overcomes another critical value $I_0 \approx 2.63\,\text{A}$. A space charge density accumulated in the electron bunch (VC) makes it unstable and forces it to divide into a few separate electron clouds at $I_0 \approx 2.63\,\text{A}$ (see Fig. 3(e)). Separate electron bunches lie approximately in the same plane in space and strongly influence on each others spatiotemporal dynamics. It is clear that the mechanism of the transition to chaos at high current values is similar to one taking place at $I_0 = 2.41\,\text{A}$ (Fig. 3(c)). The abrupt character of the last transition to chaotic dynamics is determined by the absence of a period-doubling bifurcation prior to the transition. Such abrupt process of switching of the system dynamics to chaos at high current values is conditioned by the lack of a separate weakly coupled electron structures, unlike the case of lower beam currents.

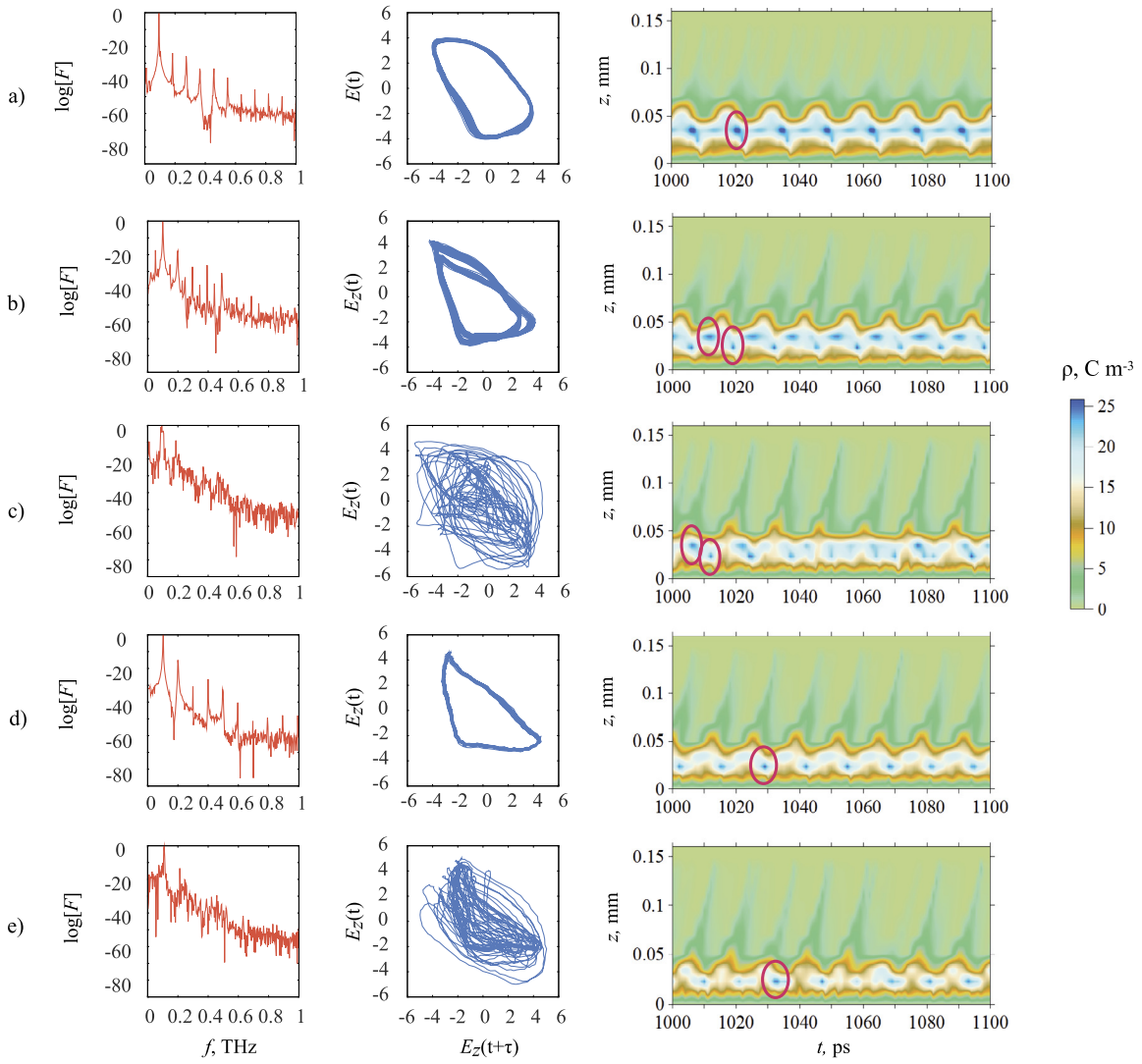

Fig. 3. Log-scaled Fourier spectra and phase portraits of longitudinal electric field E_z oscillations in the VC area (left and middle columns, respectively) and spatiotemporal distributions of electron beam space charge density $\rho(z,t)$ illustrating the processes of coherent electron structures formation (right column). These pictures are plotted for the different values of beam current: (*a*) $I_0 = 2.3$ A, $\Lambda = 0$; (*b*) $I_0 = 2.40$ A, $\Lambda = 0$; (*c*) $I_0 = 2.45$ A, $\Lambda = 0.293$; (*d*) $I_0 = 2.52$ A, $\Lambda = 0$; (*e*) $I_0 = 2.7$ A, $\Lambda = 0.41$. The delay time for phase portrait reconstruction according to Takens' theorem is $\tau = 8.3$ ps. Red ellipses highlight electron patterns. (For interpretation of the references to color in this figure legend, the reader is referred to the web version of this article.)

4. Conclusions

The obtained results reveal the basic features of nonlinear dynamics and bifurcation mechanisms in the intense electron beam with the virtual cathode in micrometer-scaled source of sub-THz electromagnetic radiation ("nanovircator"). We have found out that the system demonstrates the sequence of bifurcations (periodic regime → double-period regime → chaotic regime → periodic regime → chaotic regime) with the beam current growth. We have analyzed the physical processes responsible for the regimes switchings in the system from the viewpoint of formation and interaction of electron structures in the beam. In general, chaotization of the system dynamics is related with the appearance of additional electron bunches in the beam and their complex interaction, while simplification is the consequence of their destruction.

Due to the fact that the processes in the intense electron beam with VC depend mainly on the beam current value and on the ratios of the system sizes but not on their absolute values, the obtained results have the additional interest and may be extended to many systems with virtual cathode (not only micrometer-scaled).

The studies have been supported by the President's program (Project MK-1163.2017.2) and the Ministry of Education and Science of the Russian Federation (Projects 3.6723.2017/8.9, 3.4593.2017/6.7, 3.859.2017/4.6).

References

[1] I.S. Aranson, L. Kramer, The world of the complex Ginzburg–Landau equation, Rev. Mod. Phys. 74 (2002) 99–143.

[2] J. Bragard, F.T. Arecchi, S. Boccaletti, Characterization of synchronized spatiotemporal states in coupled non identical complex Ginzburg–Landau equations, Int. J. Bifurc. Chaos 10 (2000) 2381.

[3] Z. Tasev, L. Kocarev, L. Junge, U. Parlitz, Synchronization of Kuramoto–Sivashinsky equations using spatially local coupling, Int. J. Bifurc. Chaos 10 (4) (2000) 869–873.

[4] H.G. Schuster, Deterministic Chaos, Physik-Verlag, Weinheim, 1984.

[5] A.E. Hramov, A.A. Koronovskii, S.A. Kurkin, V.V. Makarov, M.B. Gaifullin, K.N. Alekseev, N. Alexeeva, M.T. Greenaway, T.M. Fromhold, A. Patane, F.V. Kusmartsev, V.A. Maximenko, O.I. Moskalenko, A.G. Balanov, Subterahertz chaos generation by coupling a superlattice to a linear resonator, Phys. Rev. Lett. 112 (2014) 116603.

[6] N.S. Phrolov, A.A. Koronovskii, Y. Kalinin, S.A. Kurkin, A.E. Hramov, The effect of an external signal on output microwave power of a low-voltage vircator, Phys. Lett. A 378 (2014) 2423–2428.
[7] V.N. Barabanov, A.E. Dubinov, M.V. Loiko, S.K. Saikov, V.D. Selemir, V.P. Tarakanov, Beam discharge excited by distributed virtual cathode, Plasma Phys. Rep. 38 (2) (2012) 169–178.
[8] A.M. Shigaev, B.S. Dmitriev, Y.D. Zharkov, N.M. Ryskin, Chaotic dynamics of delayed feedback klystron oscillator and its control by external signal, IEEE Trans. Electron Devices 52 (5) (2005) 790–797.
[9] V.G. Anfinogentov, A.E. Hramov, Oscillation conditions of the vircator klystron with external delayed feedback: a computer simulation, Commun. Technol. Electron. 46 (5) (2001) 546–549.
[10] Y. Kalinin, A.A. Koronovskii, A.E. Hramov, Chaotic wideband microwave oscillations in a hybrid system consisting of a traveling wave tube and a collector oscillator, Tech. Phys. 53 (5) (2008) 614–619.
[11] S. Alberti, J.-P. Ansermet, K.A. Avramides, F. Braunmueller, P. Cuanillon, J. Dubray, D. Fasel, J.-P. Hogge, A. Macor, E. de Rijk, M. da Silva, M.Q. Tran, T.M. Tran, Q. Vuillemin, Experimental study from linear to chaotic regimes on a terahertz-frequency gyrotron oscillator, Phys. Plasmas 19 (12) (2012) 123102, http://dx.doi.org/10.1063/1.4769033.
[12] L. Esaki, R. Tsu, Superlattices and negative differential conductivity in semiconductors, IBM J. Res. Dev. 14 (1) (1970) 61–65.
[13] T. Hyart, K.N. Alekseev, E.V. Thuneberg, Bloch gain in dc-ac-driven semiconductor superlattices in the absence of electric domains, Phys. Rev. B, Condens. Matter Mater. Phys. 77 (16) (2008) 165330, http://dx.doi.org/10.1103/PhysRevB.77.165330.
[14] T. Hyart, J. Alexeeva, N.V. Mattas, K.N. Alekseev, Terahertz Bloch oscillator with a modulated bias, Phys. Rev. Lett. 102 (2009) 140405.
[15] A.O. Selskii, A.E. Hramov, A.A. Koronovskii, O.I. Moskalenko, A.G. Balanov, Bifurcation phenomena in a semiconductor superlattice subject to a tilted magnetic field, Phys. Lett. A 380 (1–2) (2016) 98–105.
[16] S.A. Kurkin, A.A. Badarin, A.A. Koronovskii, A.E. Hramov, The development and interaction of instabilities in intense relativistic electron beams, Phys. Plasmas 22 (12) (2015), http://dx.doi.org/10.1063/1.4938216.
[17] A.E. Hramov, A.A. Koronovskii, S.A. Kurkin, Numerical study of chaotic oscillations in the electron beam with virtual cathode in the external non-uniform magnetic fields, Phys. Lett. A 374 (2010) 3057–3066.
[18] A.S. Shlapakovski, T. Queller, Y. Bliokh, Y.E. Krasik, Investigations of a double-gap vircator at sub-microsecond pulse durations, IEEE Trans. Plasma Sci. 40 (6) (2012) 1607–1617.
[19] R.A. Mahaffey, P.A. Sprangle, J. Golden, C.A. Kapetanakos, High-power microwaves from a non-isochronous reflecting electron system, Phys. Rev. Lett. 39 (13) (1977) 843.
[20] D.J. Sullivan, J.E. Walsh, E.A. Coutsias, Virtual cathode oscillator (vircator) theory, in: V.L. Granatstein, I. Alexeff (Eds.), High Power Microwave Sources, vol. 13, Artech House Microwave Library, 1987.
[21] L.S. Bogdankevich, A.A. Rukhadze, Stability of relativistic electron beams in a plasma and the problem of critical currents, Sov. Phys. Usp. 14 (1971) 163.
[22] A.E. Hramov, S.A. Kurkin, A.A. Koronovskii, A.E. Filatova, Effect of self-magnetic fields on the nonlinear dynamics of relativistic electron beam with virtual cathode, Phys. Plasmas 19 (11) (2012) 112101, http://dx.doi.org/10.1063/1.4765062.
[23] J. Benford, J.A. Swegle, E. Schamiloglu, High Power Microwaves, third edition, Ser. Plasma Phys., CRC Press, Taylor and Francis Group, 2016.
[24] A.E. Dubinov, I.A. Efimova, K.E. Mikheev, V.D. Selemir, V.P. Tarakanov, Hybrid microwave oscillators with a virtual cathode, Plasma Phys. Rep. 30 (6) (2004) 496.
[25] S.A. Kurkin, N.S. Frolov, A.O. Rak, A.A. Koronovskii, A.A. Kurayev, A.E. Hramov, High-power microwave amplifier based on overcritical relativistic electron beam without external magnetic field, Appl. Phys. Lett. 106 (153503) (2015) 1–5.
[26] S.A. Kurkin, A.E. Hramov, A.A. Koronovskii, Nonlinear dynamics and chaotization of virtual cathode oscillations in annular electron beam in uniform magnetic field, Plasma Phys. Rep. 35 (8) (2009) 628–642.
[27] S.A. Kurkin, A.A. Koronovskii, A.E. Hramov, Specific features of virtual cathode formation and dynamics with allowance for the magnetic self-field of a relativistic electron beam, Plasma Phys. Rep. 39 (4) (2013) 296–306.
[28] A.E. Dubinov, I.A. Efimova, Y.I. Kornilova, S.K. Saikov, V.D. Selemir, V.P. Tarakanov, Nonlinear dynamics of electron beams with a virtual cathode, Phys. Part. Nucl. 35 (2004) 251–284.
[29] S.A. Kurkin, A.A. Koronovskii, A.E. Hramov, Effect of the electron beam modulation on the sub-THz generation in the vircator with the field-emission cathode, J. Plasma Phys. 81 (2015), http://dx.doi.org/10.1017/S0022377815000252.
[30] E.N. Egorov, Y. Kalinin, A.A. Koronovskii, Y. Levin, A.E. Hramov, Analysis of the formation of structures and chaotic dynamics in a nonrelativistic electron beam with a virtual cathode in the presence of a decelerating field, J. Commun. Technol. Electron. 52 (1) (2007) 45.
[31] D.I. Trubetskov, E.S. Mchedlova, V.G. Anfinogentov, V.I. Ponomarenko, N.M. Ryskin, Nonlinear waves, chaos and patterns in microwave devices, Chaos 6 (3) (1996) 358.
[32] M. Kocan, S. Kuhn, D. Tskhakaya, J.D. Skalny, Particle simulations of the nonlinear electron dynamics in the classical Pierce diode, J. Plasma Phys. 72 (6) (2006) 851–855.
[33] D. Li, J. Zhang, X. Chen, Nonlinear dynamics of a plasma-filled diode in the presence of a magnetic field with loads, Phys. Plasmas 15 (2008) 023110.
[34] E.D. Donets, E.E. Donets, E.M. Syresin, A.E. Dubinov, I.V. Makarov, S.A. Sadovoi, S.K. Saikov, V.P. Tarakanov, Nonlinear dynamics of longitudinal structures in the electron cloud of a coaxial electron string ion source, Tech. Phys. 56 (2011) 690–696.
[35] A.E. Hramov, A.A. Koronovsky, S.A. Kurkin, I.S. Rempen, Chaotic oscillations in electron beam with virtual cathode in external magnetic field, Int. J. Electron. 98 (11) (2011) 1549–1564.
[36] A.E. Hramov, A.A. Koronovskii, V.A. Maximenko, O.I. Moskalenko, Computation of the spectrum of spatial Lyapunov exponents for the spatially extended beam-plasma systems and electron-wave devices, Phys. Plasmas 19 (8) (2012) 082302.
[37] N.S. Frolov, S.A. Kurkin, M.V. Khramova, A.A. Badarin, A.A. Koronovskii, A.N. Pavlov, A.E. Hramov, Perspective sub-THz powerful microwave generator “nanovircator” for t-rays biomedical diagnostics, Proc. SPIE 9917 (2016) 991721.
[38] P.H. Siegel, A. Fung, H. Manohara, J. Xu, B. Chang, Nanoklystron: a monolithic tube approach to THz power generation, in: 12th International Symposium on Space Terahertz Technology, 2001, pp. 81–90.
[39] H.M. Manohara, P.H. Siegel, M.J. Bronikowki, B.K. Vancil, K. Hawken, Development of a micromachined THz nanoklystron: a status report, in: IEEE Conference Record – Abstracts. The 31st IEEE International Conference on Plasma Science, ICOPS'2004, 2004, p. 421.
[40] J.H. Booske, Plasma physics and related challenges of millimeter-wave-to-terahertz and high power microwave generation, Phys. Plasmas 15 (5) (2008) 055502.
[41] R.J. Barker, E. Schamiloglu, High-Power Microwave Sources and Technologies, IEEE Press, New York, 2001.
[42] C.K. Birdsall, A.B. Langdon, Plasma Physics via Computer Simulation, Taylor and Francis Group, 2005.
[43] CST AG, User Manual, CST Particle Studio, Darmstadt, Germany, 2011.
[44] A. Taflove, S.C. Hagness, Computational Electrodynamics: The Finite-Difference Time-Domain Method, third edition, Artech House, 2005.
[45] R.W. Hockney, J.W. Eastwood, Computer Simulation Using Particles, McGraw-Hill, NY, 1981.
[46] K.S. Yee, Numerical solution of initial boundary value problems involving Maxwell's equations in isotropic media, IEEE Trans. Antennas Propag. 14 (3) (1966) 302–307.
[47] R. Courant, K. Friedrichs, H. Lewy, On the partial difference equations of mathematical physics, IBM J. Res. Dev. 11 (2) (1967) 215–234.
[48] B. Krietenstein, R. Schuhmann, P. Thoma, T. Weiland, The perfect boundary approximation technique facing the big challenge of high precision field computation, in: Proc. 19th Int. Linear Accel. Conf., 1998, pp. 860–862.
[49] M.C. Balk, Simulation possibilities of vacuum electronic devices with CST PARTICLE STUDIO, in: IEEE International Vacuum Electronics Conference (IVEC), 2008, pp. 459–460.
[50] M.C. Balk, 3D Magnetron simulation with CST STUDIO SUITE, in: IEEE International Vacuum Electronics Conference (IVEC), 2011, pp. 443–444.
[51] T. Isenlik, K. Yegin, Tutorial on the design of hole-slot-type cavity magnetron using CST particle studio, IEEE Trans. Plasma Sci. 41 (2) (2013) 296–304.
[52] S. Champeaux, P. Gouard, R. Cousin, J. Larour, 3-D PIC numerical investigations of a novel concept of multistage axial vircator for enhanced microwave generation, IEEE Trans. Plasma Sci. 43 (11) (2015) 3841–3855.
[53] S.A. Kurkin, A.A. Badarin, A.A. Koronovskii, A.E. Hramov, Higher harmonics generation in relativistic electron beam with virtual cathode, Phys. Plasmas 21 (9) (2014) 093105.
[54] A. Wolf, J. Swift, H.L. Swinney, J. Vastano, Determining Lyapunov exponents from a time series, Physica D 16 (1985) 285.